ACTIVITY ASSOCIATED WITH CORONAL MASS EJECTIONS AT SOLAR MINIMUM: SMM OBSERVATIONS FROM 1984–1986

O. C. ST. CYR

High Altitude Observatory, National Center for Atmospheric Research, Boulder, CO 80307, U.S.A.*

and

D. F. WEBB

Institute for Space Research, Boston College, Newton Center, MA 02159, U.S.A.

(Received 3 May, 1991; in revised form 2 July, 1991)

Abstract. We have examined 73 coronal mass ejections observed by the coronagraph aboard NASA's Solar Maximum Mission between 1984–1986. The goal of this study was to determine the distribution of various forms of solar activity that were spatially and temporally associated with mass ejections during solar minimum phase. For each coronal mass ejection a speed could be measured, hence, we were able to estimate a departure time of the transient from the lower corona. We then searched for other forms of solar activity that appeared within 45° longitude and 30° latitude of the mass ejection and within ± 90 minutes of its extrapolated departure time. We present the statistical results of the analysis of these 73 mass ejections, and we found that slightly less than half of the mass ejections had associations. This fraction is lower than reported by similar previous studies of Skylab and SMM 1980 coronagraph observations. We attribute the lower association rate to the large fraction of slow mass ejections detected during 1984–1986. Taken as a group, the slow mass ejections were infrequently associated with other forms of solar activity. This is the first such study to examine the association problem near the minimum phase of solar activity, but our results indicate that the distribution of the various forms of activity related to mass ejections does not appear to change at different phases of the solar cycle. For those CMEs with associations we found that eruptive prominences and soft X-ray events (especially long-decay events) were the most likely forms of activity to accompany the appearance of mass ejections. Our result strengthens the interpretation that most coronal mass ejections are the result of the reconfiguration of a magnetic field structure surrounding a prominence, leading to the destabilization and eruption of the prominence and its overlying coronal structure. This phenomenon occurs in both quiescent prominences and in prominences found in active regions.

1. Introduction

The spectacular ejection of material through the Sun's corona has been a matter of inquiry for almost two decades. Beyond a purely astrophysical interest in understanding these events, coronal mass ejections ('CMEs' or 'mass ejections' in this paper) warrant further study because of their interplanetary and geophysical consequences, so that reliable predictions of the CME occurrence can be made. Therefore, attempts to correlate the appearance of mass ejections with other more easily observed manifestations of solar activity is a worthwhile endeavor. The goal of the study reported here has been to determine the distribution of various forms of solar activity that were spatially

* The National Center for Atmospheric Research is sponsored by the National Science Foundation.

Solar Physics **136:** 379–394, 1991.

and temporally associated with the appearance of mass ejections during solar minimum phase.

The high level of light scattered in the Earth's atmosphere has restricted, to a great extent, the routine detection of coronal mass ejections to spaceborne coronagraphs. Although detected by the Naval Research Laboratory's instrument on OSO-7 (Tousey, 1973), CMEs were first routinely observed in 1973–1974 by the coronagraph aboard NASA's *Skylab* (MacQueen, 1980). Since that time two other spaceborne coronagraphs have detected several thousand mass ejections. The NRL *Solwind* white-light coronagraph aboard USAF satellite P78-1 monitored the corona from 1979 until 1985 (Howard *et al.*, 1985; Howard, Sheeley, and Michels, 1986); and the High Altitude Observatory provided the coronagraph/polarimeter aboard NASA's Solar Maximum Mission (MacQueen *et al.*, 1980). The SMM instrument obtained coronal images for seven months in 1980 and between 1984–1989. The 1984–1986 observations from the SMM coronagraph are the basis of this report.

Other forms of solar activity (e.g., prominence and filament eruptions, Hα flares, soft X-ray events, and metric II, IV radio bursts) sometimes occur near the location and at the time of mass ejections. Since coronagraphs on or near the Earth typically do not detect mass ejections directed toward the Earth, accurate predictions of geomagnetic and magnetospheric disturbances must rely on these alternate activity indicators. Statistical studies of correlated activity can yield important boundary conditions for the dynamics of CMEs and can provide the means for predicting the appearance of the coronal transients through proxy signatures.

Previous studies have concluded that prominence eruptions are the most common form of activity associated with the appearance of coronal mass ejections. This conclusion was reached by Sheeley *et al.* (1975) and Munro *et al.* (1979) based on observations by the *Skylab* coronagraph during the declining phase of solar cycle 20. In a more recent study of the association of mass ejections with other forms of solar activity, Webb and Hundhausen (1987) derived a similar conclusion using the 1980 SMM observations – data obtained during the phase of activity maximum of solar cycle 21. In this report we present analysis of a CME association study using observations obtained near the minimum phase of solar cycle 21. Preliminary results were presented by Webb and St. Cyr (1987); the X-ray characteristics of a subset of these data (consisting of 16 of the 73 CMEs studied here) were described by Harrison *et al.* (1990).

The primary motivation for this work is to expand the statistical comparison of CME-associated activity through a phase of the solar cycle never before examined–solar minimum. The solar cycle is marked by striking changes in the rates of active region appearance, flare production, and prominence eruptions. Recent results have indicated that the rate of CMEs may also track the solar activity cycle (Webb, 1991). Hence it seems reasonable to inquire whether the forms of activity associated with mass ejections also change with solar cycle phase.

There are two reasons that the 1984–1986 SMM data set is suitable for studying this question. First, there was a greatly reduced activity level during solar minimum, and this reduced the ambiguity concerning the associations of mass ejections with other forms

of activity. The result should be a much smaller fraction of accidental (i.e., incorrect) associations than in similar studies that have used data obtained at more active solar phases.

Second, the SMM instrument maintained a very high duty cycle during the collection of the data used in the study. The *Skylab* coronagraph observations extended over a duration of nine months, but they were frequently interrupted by tasks associated with the manned portion of that mission. The SMM coronagraph operated for seven months during 1980 (ending with a hardware failure in the SMM attitude control system), but the instrument's observing sequences were designed to take advantage of targets-of-opportunity by concentrating coverage on a single limb of the Sun. This mode of operation resulted in good temporal coverage of some coronal mass ejections, but a uniform depiction of the state of coronal activity was sacrificed.

SMM observations resumed in mid-1984 following the successful in-orbit repair of the spacecraft by astronauts aboard the space shuttle *Challenger*. A change in observing philosophy was instituted in the post-1984 SMM coronagraph operations, and the observing sequences were designed to acquire a more complete, synoptic sample of coronal activity. The effect has been quantified by Hundhausen *et al.* (1984) in the following manner: for the detection of mass ejections with speeds of 400 km s^{-1} or less, the *Skylab* coronagraph maintained a 32% duty cycle (i.e., daily observing efficiency, defined as one complete view of the corona during each 94 minute orbit); during 1980 the SMM coronagraph maintained a duty cycle of 38%. The *Solwind* coronagraph duty cycle was improved over *Skylab* and SMM 1980 and was estimated as 67% for 1979–1981 (Howard *et al.*, 1985). But the average SMM post-1984 daily observing efficiency was 87% (tabulated by MacQueen and St. Cyr, 1991). Thus, the 1984–1986 SMM observations represent a more complete picture of coronal activity than has been available for any previous study of the association of other forms of solar activity with the appearance of coronal mass ejections.

2. Method

Times and locations of coronal mass ejections used in this study were taken from a catalogue of SMM observations compiled by St. Cyr and Burkepile (1990). (An update and expansion of that catalogue is in progress; however, the revisions will not significantly affect the results of the study presented here.) The observations began June 8, 1984, and extended with only minor interruptions through December 7, 1986, when the failure of an onboard data storage device resulted in an extended data gap of several months.

Our method depended on measuring the radial expansion of each CME as a function of time. We attempted to find an individual feature in each mass ejection that could be identified in successive images. The most common features identified were 'loop front' or 'cavity'. The height of the chosen feature was measured in successive images and, when possible, a 'height versus time' plot was constructed for each mass ejection. Figure 1 shows a time sequence of images of a mass ejection with a frontal loop and

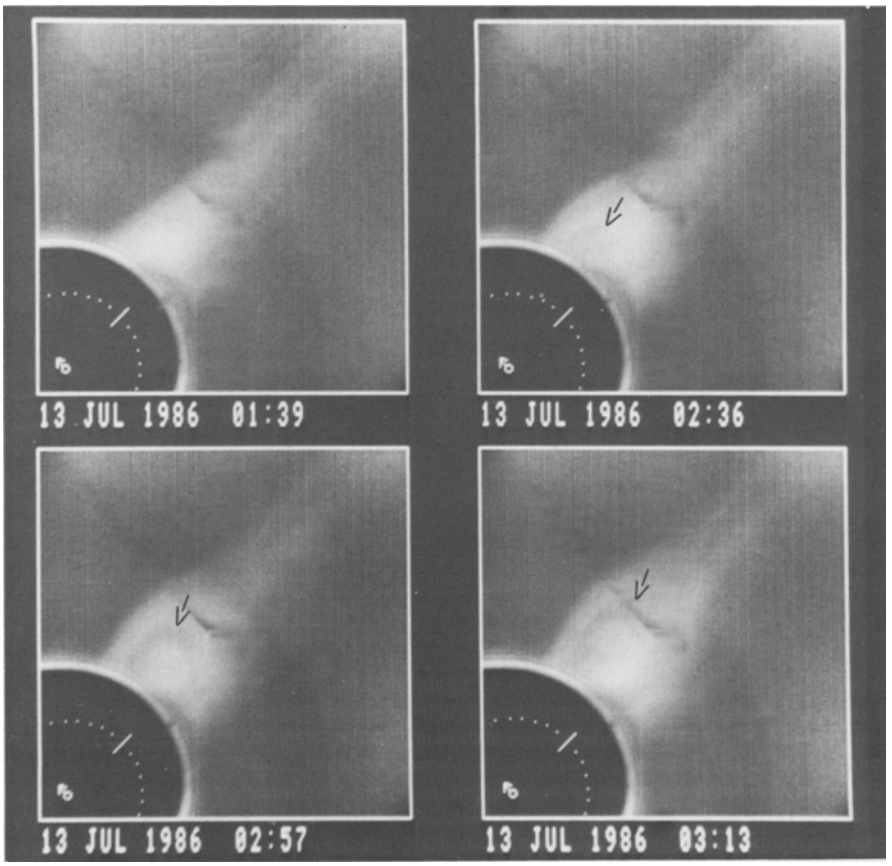

Fig. 1. Shown here is a time sequence of four images from the Solar Maximum Mission coronagraph taken on 13 July 1986 between 01:39 and 03:13 UT. The SMM instrument imaged quadrants of the corona, and all of these images were acquired through the telescope's broad band green filter (5000–5350 Å). Superposed on the shadow of the instrument's occulting disk is a dotted arc showing the size and location of the solar photosphere. The apparent direction of the Sun's north pole is indicated by the small white arrow, and a small line denotes the location of the solar equator. A pre-existing coronal streamer is seen in the first image (01:39 UT) appearing above the west limb of the Sun. At 02:36 UT a dark cavity appears in the streamer, and a black arrow has been drawn in this and subsequent images near the outermost edge of the cavity. (A bright frontal loop was also visible in these images when they were subtracted from an earlier base image.) As the dark cavity passes through the coronal streamer, a bright central core appears within the cavity. The coronal streamer was completely disrupted by the passage of the mass ejection. (For presentation purposes, selected areas within these images have been digitally 'cleaned' to remove some of the electronic artifacts that were present in all of the SMM coronagraph data.)

a cavity. The resulting height-time plot for measurements of the motion of the cavity is shown in Figure 2. The measured points on the height-time plot were fit by a linear least squares method (i.e., assuming constant speed). The linear fit yielded a speed directly, and the intersection of the line with altitude 1 $R_\odot$ produced an extrapolated departure time for the mass ejection. This extrapolation assumes that the mass ejection was in the

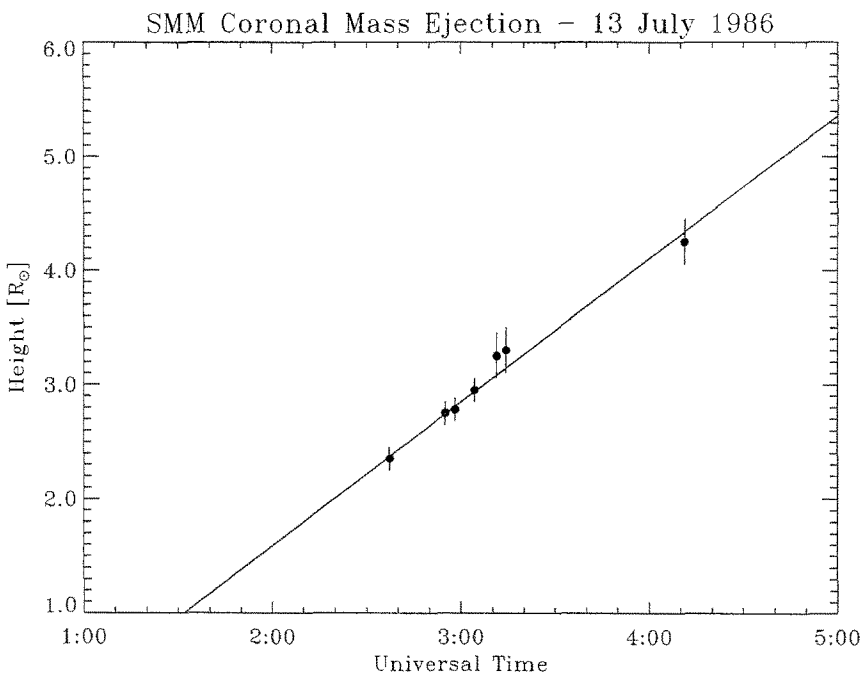

Fig. 2. The height-time plot for the coronal mass ejection of 13 July 1986. The speed of the top of the dark cavity was 237 km s^{-1} as determined from a linear least squares fit of the data points on the height-time graph shown (seven measured data points). The length of the error bars vary from ± 0.1 to ± 0.2 $R_\odot$. The extrapolated departure time for this event was 01:32 UT, determined by the intersection of the linear fit with altitude 1 $R_\odot$. Based on the linear extrapolated start time this mass ejection was associated with an Hα flare and a LDE soft X-ray event from active region 4736. The presence of the bright core within the dark cavity is taken to be evidence of prominence material in this mass ejection.

plane of the sky and that the initial location of the material comprising the mass ejection was near the solar limb (i.e., 1 $R_\odot$). In many CMEs a feature could be distinguished in more than two images, and for these cases determinations of the uncertainty in both the speed and the extrapolated departure time were obtained. Table I shows the number of CMEs detected each year and the fraction of mass ejections for which speeds could be measured. The fraction of CMEs with measured speeds during 1984–1986 (56%)

TABLE I

SMM mass ejection statistics

	1984	1985	1986	Total
Total number of mass ejections	36	42	53	131
Number of mass ejections with measured speeds	21	22	30	73 (56%)
Average speed	126 km s^{-1}	237 km s^{-1}	315 km s^{-1}	237 km s^{-1}

is comparable to that found at other phases of the solar cycle, in data obtained by the SMM instrument.

Given the apparent latitude of a mass ejection and its extrapolated departure time, we then compared tabulations of reported solar activity (see Table II) for potential associations. Types of activity considered included prominence and filament eruptions,

TABLE II

Resources searched for SMM mass ejection associations

General (ALL categories)
- *Solar Geophysical Data* (SGD)
- NOAA/USAF Solar Forecast Center Daily Reports

Erupting prominences
- SGD Mass Ejections from the Sun
- SGD Active Prominences and Filaments
- SGD Hα Solar Flares (IAU flare remarks: A, H, L, S, U, Y)
- Mauna Loa Solar Observatory Hα prominence monitor film
- Mauna Loa Solar Observatory Activity Reports (D. Sime, private communication)
- Haleakala Solar Observatory (M. McCabe, private communication)
- NOAA/SEL listing of disappearing filaments (J. Joselyn, private communication)
- Kitt Peak National Observatory (K. Harvey, private communication)
- Big Bear Solar Observatory (S. Martin, private communication)
- Ottawa River Solar Observatory (V. Gaizauskas, private communication)

Hα flares
- SGD Hα Solar Flares
- Big Bear Solar Observatory (S. Martin, private communication)
- Ottawa River Solar Observatory (V. Gaizauskas, private communication)
- USAF SOON Hα monitor film archive

X-ray events
- NOAA GOES 1–8 Å light curves
- SMM XRP data (G. Slater, R. Harrison, D. Zarro, K. Smith, private communication)
- SMM HXRBS data (Dennis *et al.*, 1988)

Metric radio type II, IV events
- SGD Solar Radio Emission (Spectral Observations)
- Clark Lake Radio Observatory (N. Gopalswamy, private communication)

Hα flares, soft X-ray events, and metric II, IV radio bursts. The selection of solar activity data types and the method of their collection were intentionally patterned after Munro *et al.* (1979) and Webb and Hundhausen (1987). Hα subflares have been treated slightly differently in each of these studies; in our study we have only included them as 'special cases', discussed in Section 3.2.

The temporal and spatial criteria described by Webb and Hundhausen (1987) were employed to determine if reported solar activity could be reasonably associated with a given mass ejection. These criteria required that: (1) the reported activity occurred within $\pm$ 90 minutes of the extrapolated departure time; (2) the latitude of the reported activity occurred within $\pm 30°$ of the apparent latitude of the mass ejection; and (3) the

longitude of the activity was within 45° of the limb where the CME appeared. Activity was assumed to be unassociated if it did not meet all of these criteria. (Webb and Hundhausen (1987) used more restrictive spatial and temporal criteria and determined a 'confidence level' of association for each CME, but our criteria correspond to the associations considered in their final statistics.)

There are some qualifications to the process of associating other forms of activity with the appearance of mass ejections, and we refer the reader to MacQueen (1985), Webb and Hundhausen (1987), and Harrison and Sime (1989) for further discussion. However, for completeness we note the following assumptions and limitations that could affect the derived mass ejection launch time:

(a) The SMM images (or similar images dependent on the Thomson scattering process) provide plane-of-the-sky measurements only – no corrections for projection effects have been made – thus the speeds may have been underestimated. (Note, however, that the true altitude of the CME has also been underestimated, and this largely compensates for any systematic error in the extrapolated start time due to the uncorrected speed.)

(b) Initiation times were determined through a least-squares linear extrapolation. We have ignored effects due to acceleration, which must have taken place as the mass ejection formed, usually beneath the shadow of the instrument's occulting disk. If the CME were subjected to a gradual acceleration over a long period, then the actual time of the onset of this acceleration could be appreciably earlier than the linearly extrapolated time.

(c) Initiation times were determined by extrapolating the height-time measurements inward to a height of 1 $R_\odot$. If the disturbance actually originated at an altitude higher than 1 $R_\odot$ (as is the case in some CMEs), then the true launch time would be later than that deduced by the linear extrapolation. On the other hand, if the CME was associated with activity located on the disk of the Sun, away from the limb, then the true launch time could be earlier than the extrapolated time.

For mass ejections of average speed or greater, corrections to the extrapolated initiation times would be small compared to the $\pm$ 90 minute window. In contrast, the corrections for slow mass ejections could be quite significant, but we will demonstrate in Section 4 that these uncertainties did not materially alter the conclusions reached in this study.

3. Results

3.1. Overall results

In Table III we show that for the 73 mass ejections with speed measurements, 34 (47%) could be associated with other forms of solar activity using the criteria described above. In this tally we have not differentiated between mass ejections with single or multiple associations, and we will describe those minor differences below. For the 1984–1986 CMEs with associations, we found agreement with the Munro *et al.* (1979) and Webb

TABLE III

SMM mass ejection associations (no special cases)

	1984	1985	1986	Total
Number of mass ejections with measured speeds	21	22	30	73
Number of mass ejections with associations	10	7	17	34 (47%)
For the 34 mass ejections with associations				
Erupting prominences	9	6	11	26 (76%)
Hα flares	2	2	5	9 (26%)
X-ray events	4	6	15	25 (74%)
Radio II, IV events	1	2	4	7 (21%)

and Hundhausen (1987) studies on the percentages of mass ejections in each activity category. 'Eruptive prominences' comprised the largest category of associated activity (about $\frac{3}{4}$), and this included reports of erupting prominences at the limb or disappearing filaments on the solar disk, sprays, bright surges on the limb, and reports of mass ejecta associated with Hα flares (IAU system flare remarks: A, H, L, S, U, Y; as described in the supplement to *Solar-Geophysical Data Explanation of Data Reports*, No. 450, February 1982).

As shown in Table III, a similar fraction of the mass ejections were correlated with X-ray events. Our primary source of information for soft X-ray activity was the GOES 6-hour, whole Sun, 1–8 Å light curves provided by NOAA's Space Environment Lab. A secondary source of information was the XRP instrument aboard SMM. Since the GOES detector observed the entire Sun without spatial resolution, the location of the source of X-ray events was not available from that instrument alone. Therefore, in order to consider a GOES event as being rigorously associated with a mass ejection, we required either: (1) a groundbased Hα report identifying the location of the GOES event or, (2) an identification of the X-ray site by the SMM XRP instrument. The XRP instrument could spatially resolve X-ray sources (Acton *et al.*, 1980), but its more limited field-of-view (typically four arc minutes) compared to GOES precluded complete coverage of X-ray activity.

Most metric radio II, IV bursts were also reported without spatial resolution. However, the Clark Lake Radio Observatory was able to provide locations of radio bursts observed there. When these reports met the criteria described in Section 2, then these have also been taken as valid associations.

Hα flares (26%) and metric radio II, IV bursts (21%) were much less frequently associated with the departure times of CMEs. In further agreement with the previous studies, we found no Hα flare-only mass ejection associations. Of the 34 associated mass ejections, there were nine CMEs that had only a single form of activity (6 in 1984; 1 in 1985; 2 in 1986). In eight out of these nine cases the single association was 'eruptive

prominence', a result that re-emphasizes the important relationship of this activity to the appearance of coronal mass ejections.

3.2. 'SPECIAL CASES'

Among the 39 'unassociated' mass ejections there were numerous candidates for consideration as 'special cases'. These CMEs did not meet the rigorous criteria outlined above, but upon careful examination of individual cases we were compelled to include some mass ejections in addition to those shown in Table III. Also, the consideration of 'special cases' facilitates comparison with similar tables in Webb and Hundhausen (1987). In this section we describe the justification for inclusion of these 'special cases' and present the tabulated statistical results which include them. We will address their significance in Section 4.

The first 'special case' we used was described in Webb and Hundhausen (1987) who noted that the inclusion of an Hα filter in the SMM instrument allowed the detection of neutral hydrogen in the coronagraph field-of-view during 1980. The existence of this cool, presumably chromospheric material was frequently detected in coronal mass ejections, taking the form of a 'central bright region', or CBR, within the expanding CME front (see Figure 1). Although coronagraph Hα images were not obtained for each CME, Webb and Hundhausen (1987) argued that the appearance of a central bright region within a mass ejection was *de facto* evidence of prominence material. Therefore, they admitted mass ejections with CBRs to the SMM 1980 association list as 'special cases', with the associated activity being an eruptive prominence.

The second 'special case' concerned CMEs that satisfied the temporal criterion but did not meet the spatial (longitude) criterion described in Section 2. Several mass ejections appeared to be associated with activity occurring near Sun center, thus violating the 'within 45° of the limb' criterion. However, examples of CME detection far from the limb have been detailed in St. Cyr and Hundhausen (1988). To strengthen the justification for this 'special case' we note that 'episodes' of mass ejections were clearly associated with the passage of some active regions across the solar disk. For example, during 1986, 61% of the mass ejections used in this study (33 of 54) occurred during only three solar rotations (Carrington rotation numbers 1771, 1777, and 1781). Because of the lack of other activity and the apparent coincident timing, these episodes were clearly related to the passage of active regions across the visible disk of the Sun. Mass ejections could be reasonably associated with bursts of activity from these regions even when they were near the Sun's central meridian.

A third 'special case' arose from the complete exclusion of Hα sub-flares as rigorously associated activity from the SMM 1980 study. The exclusion was justified in the earlier study because of the high level of solar activity. We do not believe that this restriction was appropriate for solar minimum conditions, therefore we have included Hα sub-flares as 'special case' flare associations.

Finally, there were a few mass ejections for which the timing of either a GOES X-ray event or a metric radio II, IV burst coincided with the extrapolated departure time, but no information was available on the location. Although the X-ray and radio events were

(for the most part) detected by full-disk instruments, such close agreement in timing without spatial information has frequently been considered valid evidence of association, so we have also designated these as 'special cases' of associations. These CMEs thus could have been considered as having only a single association, but without further specific information on their location we chose to include them only as 'special cases'.

We have tabulated the number of mass ejections admitted in each 'special case' category, and we show in Table IV the results of combining these cases with the CMEs in Table III. With the inclusion of these 'special cases' the fraction of CMEs with associations increased to 77% (56 of 73).

TABLE IV

SMM mass ejection associations (includes special cases)

	1984	1985	1986	Total
Number of mass ejections with measured speeds	21	22	30	73
Number of mass ejections with speed and CBR[a]	11	5	22	38 (52%)
Number of mass ejections with associations (including special cases)	16	13	27	56 (77%)
Reason for special cases				
CBR in SMM data	6	3	10	19
Longitude/latitude	–	2	3	5
Sub-flare	2	3	1	6
X-ray or radio only	–	2	3	5
For the 56 mass ejections with associations				
Erupting prominences	15	10	24	49 (88%)
Hα flares	4	7	8	19 (34%)
X-ray events	5	10	20	35 (63%)
Radio II, IV events	1	5	7	13 (23%)

[a] CBR = central bright region.

4. Discussion

4.1. General comments

Results from this study have not addressed the question of 'timing' in the appearance of coronal mass ejections or the cause-effect relationship between other forms of activity and mass ejections. Resolution of that problem requires adequate knowledge of the acceleration of a CME through the lower corona in order to compare the initiation of the mass ejection with, for example, the coincidence of a soft X-ray burst. Indeed, the goal of our study has been limited to determining the statistical likelihood that various forms of solar activity occur in approximate spatial and temporal coincidence with the appearance of coronal mass ejections at solar minimum phase.

Such an attempt to refine the timing of the initiation of CMEs and the commencement of X-ray activity has been reported by Harrison *et al.* (1990). Based on a subset of 16 CMEs from 1985–1986 SMM coronagraph and soft X-ray observations (the CME Onset program), those authors concluded that coronal mass ejections were 'strongly associated with active regions'. In our study of the complete mass ejection data set, we found 21 out of the 34 CMEs with associations (representing 62%, 'special cases' not included) could reasonably be related to activity from numbered active regions. The remaining 13 mass ejections were associated with prominence or filament eruptions outside of any active regions. Consideration of the additional 'special cases' yielded only 48% of the 56 mass ejections possibly related to active regions. The apparent disparity between the Harrison *et al.* (1990) statement and our conclusion can be explained by the observing sequences used in the CME Onset program. Those authors noted that mass ejections in their study were mostly constrained to active region observations, and they allowed that 'this scheme may produce a bias against CMEs which may not involve active regions'.

Many researchers have concluded that 'long decay' soft X-ray events (LDEs) are statistically associated with prominence eruptions and mass ejections (e.g., Sheeley *et al.*, 1983). Therefore, we have examined the nature of the GOES soft X-ray events that accompanied the 1984–1986 SMM mass ejections with associations. We determined whether or not the X-ray event was an LDE based on the criterion used by Webb and Hundhausen (1987): an associated 1–8 Å event was defined to be an LDE if the time for the flux to decay to e^{-1} of the peak was greater than 12 minutes. Using this criterion almost *all* of the soft X-ray events that were associated with mass ejections (31 of 35, including 'special cases') were LDEs.

The association of metric type II, IV bursts with coronal mass ejections has been addressed by several studies. Using *Skylab* observations, Gosling *et al.* (1976) found that these radio bursts were associated with mass ejections traveling faster than 400 km s^{-1}, and they concluded that these high-speed CMEs drove shocks through the corona ahead of the ejection, producing the radio burst. Sheeley *et al.* (1984) reached a similar conclusion based on a study of metric type II bursts associated with *Solwind* CMEs. In fact, we are aware of only a single report of a 'slower' mass ejection associated with a metric II, IV radio burst (Kundu *et al.*, 1989), and that CME was estimated to be traveling ≈ 240 km s^{-1}. We have investigated the mass ejections associated with metric radio II, IV bursts in the 1984–1986 SMM observations. The average speed for the seven mass ejections with metric radio II, IV burst associations was 487 km s^{-1}, and that average increased to 594 km s^{-1} when the six 'special cases' were included. In fact, with a single exception, all such associated radio bursts were related to mass ejections traveling 350 km s^{-1} or greater. This was true for both the seven radio bursts associated by the rigorous criteria and the additional six bursts considered as 'special cases'. The sole exception was a mass ejection that occurred February 22, 1985, and was traveling 160 km s^{-1}.

We have also examined the relationship of associated activity to two other mass ejection properties – widths and morphology – and we briefly describe these results. The

results did not change with the inclusion of the 'special cases', so quantitative values have been determined using mass ejection associations found in Table III. An angular width can usually be obtained for each mass ejection and has been generated by the method described in Webb (1987). The width for each CME was determined by locating the position angles of the two bright sides of the ejection at the lowest altitude where reliable measurements could be made (typically 2.0 to 3.0 $R_\odot$). The measurements were made when the features had extended to their maximum width and should be accurate to $\pm 5°$. We found virtually no difference between average widths of mass ejections with associations (41°) and those without association (42°). Moreover, these values agree with the 42° average described in St. Cyr and Burkepile (1990) for all 131 mass ejections observed by SMM during 1984–1986. We conclude that the average width of mass ejections is independent of the presence or absence of activity associated with their origin.

A second property that can be readily discerned is the morphological appearance of the CME. Usually one can determine the presence or absence of a 'frontal loop' and of a central bright region in each mass ejection. The appearance of a dark cavity with surrounding bright loop and embedded bright core (identified as CBR in Section 3.2) was described by Hundhausen (1988) as common features of many SMM mass ejections (as shown in Figure 1). In the complete sample of 131 SMM mass ejections detected during 1984–1986, 57% possessed a frontal loop and 35% had a central bright region. Considering the subset of 34 mass ejections with associations, 91% possessed a frontal loop; whereas 64% of the 39 mass ejections without association displayed this feature.

A larger difference between those CMEs with association and those without association was obtained when we considered the presence or absence of central bright regions. Of the 34 mass ejections with associations, 68% had central bright regions; whereas only 36% of the 39 CMEs without associations possessed this feature. This should not be surprising, since we considered a central bright region in a mass ejection to be evidence of prominence material (see Section 3.2). Nonetheless, for the 34 CMEs with associations, there was not a one-to-one correspondence of eruptive prominence reports to central bright regions. In fact, about $\frac{1}{3}$ of the eruptive prominences detected by groundbased observers did not result in distinguishable central bright regions in the resulting mass ejections (10 of 26 CMEs).

In Table V we compare the distribution of CMEs with associations during 1984–1986 with values for *Skylab* (Munro *et al.*, 1979) and for the 1980 observations by SMM (Webb and Hundhausen, 1987). This table demonstrates a reasonably consistent distribution by form of associated activity throughout the three epochs studied. We believe that the only significant discrepancy is the smaller fraction of 1984–1986 mass ejections that were associated with other forms of activity when compared to the two previous studies. The number of associated mass ejections in 1984–1986 became similar to the previous studies only by the admission of a large number of 'special cases' to our study. (For comparison we note that the 38 associated CMEs in the SMM 1980 study were increased by only 9 'special cases'.) The lower association rate was not anticipated, but

TABLE V

Comparison of associations (no special cases)

	1973–1974 (Skylab)	1980 (SMM)	1984–1986 (SMM)
Number of mass ejections with measured speeds	40[a]	58	73
Average speed	470 km s^{-1}	340 km s^{-1}	237 km s^{-1}
Number of mass ejections with associations	34 (85%)[a]	38 (66%)	34 (47%)
Distribution of associations			
Erupting prominences	31 (91%)	26 (68%)	26 (76%)
Hα flares	13 (38%)	14 (37%)	9 (26%)
X-ray events	16 (47%)	29 (76%)	25 (74%)
Radio II, IV events	14 (41%)	12 (32%)	7 (21%)

[a] See Webb and Hundhausen (1987) for discussion of Skylab CME speed measurements and associations.

we propose the following explanation for this result when compared to previous work. We note that the average speed of mass ejections in 1984–1986 was much lower than in either 1973–1974 or 1980. Slow CMEs were seldom associated with other forms of solar activity, and we discuss this point below.

4.2. Mass ejections with very slow speeds

Although a slow mass ejection remained in the SMM coronagraph's field-of-view for a longer time and thus a better measurement of its speed could be made, the interval between the linearly extrapolated initiation of the CME and its appearance in the field-of-view was very long. As seen in Table I, the average speed of mass ejections used in this study was 237 km s^{-1}. The (annual) average speed was lowest in 1984 and increased as cycle 22 activity began to appear during 1985–1986. The preponderance of slow CMEs during 1984–1986 can be demonstrated by comparing the average speed of mass ejections during this period with other reports. For *Skylab* the average speed of mass ejections was 470 km s^{-1} (Gosling *et al.*, 1976); the average CME speed at solar maximum based on Solwind coronagraph measurements was 470 km s^{-1} (Howard *et al.*, 1985); and the 1980 CME observations by SMM had an average speed of 340 km s^{-1} (see Kahler, 1987).

The effect of the slow CMEs on this statistical analysis was striking. The average speed for the 34 mass ejections with rigorously associated activity was 290 km s^{-1}; but the average speed for the 39 unassociated mass ejections was only 195 km s^{-1}. In tallying the 24 CMEs with speed greater than the 237 km s^{-1} average, we found that 71% had associations.

Considering the subset of the slowest CMEs, in 1980 there were eight SMM mass ejections traveling less than 50 km s^{-1}, and only one could be associated with other activity (Webb, 1987). In 1984–1986 there were 15 CMEs with speeds less than 50 km s^{-1}, and again only one had a rigorous association (although half of the group

were admitted as 'special cases' due to the presence of either CBR or a sub-flare). Even when the temporal window was doubled from $\pm$ 90 minutes to $\pm$ 180 minutes, no additional slow mass ejections in 1984–1986 were found with reliable associations. We thus believe that the concern raised in Section 2 about corrections to the extrapolated initiation time due to undetected acceleration or departure height variations is not a significant factor in determining associations for the slow mass ejections.

Wagner (1984) also noted that slow-moving coronal mass ejections were poorly associated with other activity, but he speculated that these represented a separate physical class of coronal transients. He based this conjecture on the slow speed of these mass ejections, their morphology as 'filled bottles', and changes in their latitude distribution at different solar cycle phases. The 1984–1986 SMM observations greatly increased the number of slow mass ejections available for study. In agreement with Webb and Hundhausen (1987) and in contrast to Wagner (1984), we found no systematic morphological characteristics in the slow mass ejections that distinguished them from the general population of CMEs; however, the average angular width of this subset of 15 CMEs was 28°, somewhat smaller than the average of the complete sample described above. Slightly more than half of the slow CMEs had a frontal loop, and one-third possessed a central bright region. Both fractions are similar to the larger subset of mass ejections without associations. One further difference with Wagner's conjecture was our finding that the slow CMEs between 1984–1986 followed the known distribution in apparent latitude for all mass ejections over the solar cycle (see Kahler, 1987). We speculate that the slow mass ejections are poorly associated simply because any Hα, X-ray, and radio signatures accompanying the ejections are weak and lie below the sensitivity threshold of instruments presently used in synoptic solar observations. This speculation is based on an assumption that the speed of a mass ejection is proportional to the intensity of associated activity, but this conjecture has not yet been proven.

5. Summary

Using observations near the minimum phase of solar cycle 21, we have extended earlier work on the statistical association of coronal mass ejections with other forms of solar activity. During the solar minimum period from 1984–1986, the number of solar coronal mass ejections with reliable associations was 47%, a lower fraction than found by two previous studies performed at other phases of the solar activity cycle. We believe that this was due to an abundance of very slow mass ejections which, taken as a class, were poorly associated with other detectable forms of solar activity.

For the CMEs with associations, eruptive prominences and soft X-ray long decay events were the most likely form of accompanying activity. While some mass ejections were related to activity associated with numbered active regions, our result strengthens the conclusion that it is the eruption of prominence structures within those active regions that is the common factor in the appearance of coronal mass ejections. This conclusion is augmented by the recognition that many mass ejections can be associated with prominences outside of active regions, and that typically Hα flares are *not* associated

with CMEs. The metric radio II, IV bursts were also less frequently associated with the general population of CMEs. However, in agreement with previous studies, we demonstrated that these radio bursts appear preferentially associated with the subset of mass ejections traveling 350 km s^{-1} or more.

Only with the admittance of a large number of 'special case' CMEs did the fraction of associations become similar to the *Skylab* and SMM 1980 studies. However, the inclusion of these special cases did not significantly change the fraction of associations found for each form of activity. From our analysis of other mass ejection properties we found no difference in the average angular widths between the subsets of mass ejections with associations and those without. Also, nearly all mass ejections that could be rigorously associated possessed 'frontal loops'; but the appearance of this feature did not guarantee that an association would be found. The appearance of a central bright region in the mass ejection increased the probability that an eruptive prominence report would be found. However, the correlation between detections of eruptive prominences by groundbased observers and the appearance of a CBR in a mass ejection was not one-to-one.

Our statistical result strengthens the interpretation that most coronal mass ejections are the result of the restructuring of a magnetic field configuration that often includes a prominence, leading to the destabilization and eruption of the field, including the overlying coronal structure and the embedded prominence. This phenomenon occurs in both quiescent prominences and in those found in active regions.

Acknowledgements

We thank A. Hundhausen at the High Altitude Observatory, E. Cliver at the Air Force Geophysics Lab., and S. Kahler at Boston College for helpful comments concerning this manuscript. Others who have contributed directly to the collection and analysis of the observations include: J. Burkepile, A. Stanger, S. Beck, D. Kobe, R. Lee, E. Einfalt, and those individuals who have been mentioned in Table II. Work by DFW on this study was supported at Emmanuel College and at Boston College by the Space Physics Division of GL under contracts AF19628–87-K-0033 and AF19628–90-K-0006. The High Altitude Observatory directed the design and manufacture of the SMM coronagraph by Ball Aerospace. Instrument operations and data analysis have been funded under NASA contract S-04167D to HAO.

References

Acton, L. W., Culhane, J. L., Gabriel, A. H. and 21 co-authors: 1980, *Solar Phys.* **65**, 53.

Dennis, B. R., Orwig, L. E., Kiplinger, A. L., Schwartz, R. A., Gibson, B. R., Kennard, G. S., Tolbert, A. K., Biesecker, D. A., Labow, G. J., and Shaver, A.: 1988, *The Hard X-Ray Burst Spectrometer Event Listing 1980–1987*, NASA Tech. Mem. 4036.

Gosling, J. T., Hildner, E., MacQueen, R. M., Munro, R. H., Poland, A. I., and Ross, C. L.: 1976, *Solar Phys.* **48**, 389.

Harrison, R. A. and Sime, D. G.: 1989, *Astron. Astrophys.* **208**, 274.

Harrison, R. A., Hildner, E., Hundhausen, A. J., Sime, D. G., and Simnett, G. M.: 1990, *J. Geophys. Res.* **95**, 917.

Howard, R. A., Sheeley, N. R., Jr., and Michels, D. J.: 1986, in R. G. Marsden (ed.), 'The Solar Cycle Dependence of Coronal Mass Ejections', *The Sun and the Heliosphere in Three Dimensions*, D. Reidel Publ. Co., Dordrecht, Holland, pp. 107–111.

Howard, R. A., Sheeley, N. R., Jr., Koomen, M. J., and Michels, D. J.: 1985, *J. Geophys. Res.* **90**, 8173.

Hundhausen, A. J.: 1988, in V. J. Pizzo, T. E. Holzer, and D. G. Sime (eds.), 'The Origin and Propagation of Coronal Mass Ejections', *Proceedings of the Sixth International Solar Wind Conference*, NCAR/TN-306 + PROC, pp. 181–214.

Hundhausen, A. J., Sawyer, C. B., House, L., Illing, R. M. E., and Wagner, W. J.: 1984, *J. Geophys. Res.* **89**, 2639.

Kahler, S.: 1987, *Rev. Geophys.* **25**, 663.

Kundu, M. R., Gopalswamy, N., White, S., Cargill, P., Schmahl, E. J., and Hildner, E.: 1989, *Astrophys. J.* **347**, 505.

MacQueen, R. M.: 1985, *Solar Phys.* **95**, 359.

MacQueen, R. M.: 1980, *Phil. Trans. Roy. Soc. London* **A297**, 605.

MacQueen, R. M. and St. Cyr, O. C.: 1991, *Icarus* **90**, 96.

MacQueen, R. M., Csoeke-Poeckh, A., Hildner, E., House, L. L., Reynolds, R., Stanger, A., TePoel, H., and Wagner, W. J.: 1980, *Solar Phys.* **65**, 91.

Munro, R. H., Gosling, J. T., Hildner, E., MacQueen, R. M., Poland, A. I., and Ross, C. L.: 1979, *Solar Phys.* **61**, 201.

Sheeley, N. R., Jr., and 12 co-authors: 1975, *Solar Phys.* **45**, 377.

Sheeley, N. R., Howard, R. A., Koomen, M. J., and Michels, D. J.: 1983, *Astrophys. J.* **272**, 349.

Sheeley, N. R., Stewart, R. T., Robinson, R. D., Howard, R. A., Koomen, M. J., and Michels, D. J.: 1984, *Astrophys. J.* **279**, 839.

St. Cyr, O. C. and Burkepile, J. T.: 1990, *A Catalogue of Mass Ejections Observed by the Solar Maximum Mission Coronagraph*, NCAR Technical Note, NCAR/TN-352 + STR.

St. Cyr, O. C. and Hundhausen, A. J.: 1988, in V. J. Pizzo, T. E. Holzer, and D. G. Sime (eds.), 'On the Interpretation of 'Halo' Coronal Mass Ejections', *Proceedings of the Sixth International Solar Wind Conference*, NCAR/TN-306 + PROC, pp. 235–241.

Tousey, R.: 1973, in M. J. Rycroft and S. K. Runcorn (eds.), *The Solar Corona*, Space Research XIII, Akademie-Verlag, Berlin, p. 713.

Wagner, W. J.: 1984, *Ann. Rev. Astron. Astrophys.* **22**, 267.

Webb, D. F.: 1987, *Table of Solar Activity Associated with Coronal Mass Ejections Observed by the SMM Coronagraph/Polarimeter in 1980*, NCAR Technical Note, NCAR/TN-297 + STR.

Webb, D. F.: 1991, *Adv. Space Res.* **11**, 37.

Webb, D. F. and Hundhausen, A. J.: 1987, *Solar Phys.* **108**, 383.

Webb, D. F. and St. Cyr, O. C.: 1987, *Bull. Am. Astron. Soc.* **19**, 936.